Nuclear Instruments and Methods in Physics Research A 654 (2011) 532–538

Contents lists available at ScienceDirect

Nuclear Instruments and Methods in Physics Research A

journal homepage: www.elsevier.com/locate/nima

Study of TOF PET using Cherenkov light

S. Korpar [a,b], R. Dolenec [b,*], P. Križan [c,b], R. Pestotnik [b], A. Stanovnik [d,b]

[a] Faculty of Chemistry and Chemical Engineering, University of Maribor, Maribor, Slovenia
[b] Jožef Stefan Institute, Jamova cesta 39, SI-1000 Ljubljana, Slovenia
[c] Faculty of Mathematics and Physics, University of Ljubljana, Ljubljana, Slovenia
[d] Faculty of Electrical Engineering, University of Ljubljana, Ljubljana, Slovenia

ARTICLE INFO

Article history:
Received 30 March 2011
Received in revised form
23 May 2011
Accepted 5 June 2011
Available online 17 June 2011

Keywords:
Time-of-flight
PET
Cherenkov radiation
Microchannel plate photomultipliers
Lead fluoride
Lead tungstate

ABSTRACT

This work investigates the possibilities of improving the measurements of arrival time difference of the two 511 keV photons arising from annihilation of a positron in positron emission tomography (PET). The new technique of detecting the prompt Cherenkov light, produced by absorption of the annihilation photon in a suitable crystal, could considerably improve the image quality. A simple apparatus with PbF_2 crystals and microchannel plate photomultipliers (MCP PMTs) has been constructed and coincidence resolutions of 71 ps FWHM and 95 ps FWHM have been achieved with 5 and 15 mm thick crystals, respectively. Simulation calculations are in agreement with the experimental findings.

1. Introduction

Positron emission tomography (PET) is an important modality in medical imaging, used to detect the position of tumors and to observe biochemical processes in the body. The contrast of images obtained with PET can be significantly improved by measuring the time difference between the arrival of two annihilation photons. The amount of improvement in the image depends on the time resolution, which is usually limited by the decay time of the scintillations and the time resolution of the photodetector. Using the microchannel plate photomultiplier, a photodetector with excellent timing [1,2], to detect prompt Cherenkov photons, has the potential of providing a big improvement in the time-of-flight resolution. For the upgrade of the Belle II detector, we have already investigated how a MCP PMT could be used for detection of Cherenkov photons, produced by pions or kaons in an aerogel radiator and in the entrance window of a MCP PMT [3]; some other studies of time-of-flight measurements for charged particles also showed very good performance [4,5]. In the present work we consider the possibility of using a very fast MCP PMT to measure the time-of-flight difference of 511 keV annihilation gammas. Some early studies of this approach have achieved time-of-flight resolutions of 170 ps FWHM [6], 183 ps FWHM (our first study [7]) and 250 ps FWHM [8]. In the present study we have considerably improved the timing resolution and found a good agreement with Monte Carlo simulation.

Below, we first describe the principles of the detection method. In the third section we present the experimental apparatus and then we discuss the results of measurements of time resolution for two coincident 511 keV gamma photons absorbed in PbF_2 crystals. Next, we compare our measurements with simulation calculations, which also included a study with $PbWO_4$ crystals in order to investigate possible improvements of the design. The last section contains a short discussion of the results and some conclusions.

2. Detection method

To obtain Cherenkov photons for time-of-flight measurements of 511 keV gammas, we need a material in which the annihilation gammas efficiently transfer their energy to electrons. Photons with energy of 511 keV interact with matter either through the photoelectric effect or by Compton scattering. Here the former is preferred, since all of the photon's energy are deposited in one interaction, which results in a photoelectron with the maximum kinetic energy possible. The material used as a Cherenkov radiator should have a high index of refraction i.e. low Cherenkov threshold, so that many electrons are produced above the Cherenkov threshold. It should also have a high stopping power for 511 keV gammas. All this suggests a high density and high-Z material. Also, the material must have good transmission for light in the

* Corresponding author. Tel.: +386 1 477 3702; fax: +386 1 477 3166.
E-mail address: rok.dolenec@ijs.si (R. Dolenec).

0168-9002/$ - see front matter © 2011 Elsevier B.V. All rights reserved.
doi:10.1016/j.nima.2011.06.035

blue to near UV region, where most of the detectable Cherenkov photons are produced. Most promising candidates are high lead content crystals, such as lead fluoride (PbF_2) and lead tungstate ($PbWO_4$). Some of their properties are summarized in Table 1.

Even though the Cherenkov photons are produced promptly, a significant contribution to the timing resolution can be expected from the Cherenkov photon travel time spread in the crystal. A very simple estimate of the time resolution can be obtained by considering the difference between the shortest and the longest time from the moment that the 511 keV gamma enters the crystal to the moment that the resulting Cherenkov photon reaches the photodetector. The shortest time is obtained, when the gamma enters the crystal perpendicularly to the entry surface and causes the production of a Cherenkov photon at the very end of the crystal. Assuming no reflections from the crystal sides, the longest time is obtained for a gamma, which is absorbed as soon as it enters the crystal and a Cherenkov photon, which travels to the photodetector under a large angle relative to the entry surface normal. In the case of our measurements this angle is limited by detector geometric acceptance and amounts to approximately 30°. For a crystal with thickness $d=15$ mm and index of refraction of $n=1.8$ (PbF_2), the difference between the shortest time, $t_{min}=d/c_0=50$ ps and the longest time, $t_{max}=(d/\cos 30^\circ)(n/c_0)=104$ ps, is 54 ps. This would result in a r.m.s. spread of about $\sigma\approx 20$ ps. If we combine this rough estimate with the typical photon detection time resolution ($\sigma\approx 20$ ps), we see that the best coincidence timing resolution we can expect is $\sigma\approx\sqrt{2*(20^2+20^2)}$ ps $=40$ ps, which translates to r.m.s. ≈ 6 mm in spatial resolution along the line of response.

The above analysis suggests that considerable benefits and improvements of PET image quality may be obtained by detecting annihilation photon coincidences via the prompt Cherenkov light they produce in suitable radiators. In order to experimentally verify these estimates we have constructed a simple apparatus, with which we have confirmed the optimistic expectations.

Table 1
Properties of two promising Cherenkov radiators [9–13].

	PbF_2	$PbWO_4$
Index of refraction ($\lambda=400$ nm)	1.8	2.3
Density (g/cm^3)	7.77	8.28
Cherenkov threshold for e^- (keV)	104	56
Optical transmission cutoff wavelength (nm)	250	350
Scintillation light yield (photons/MeV)	–	200
Scintillation decay time (ns)	–	6/30
Scintillation emission peak (nm)	–	440/530

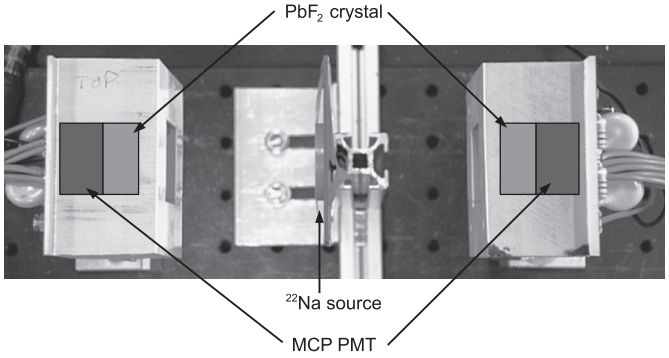

Fig. 1. The experimental set-up: two Hamamatsu 16 channel MCP PMTs coupled to lead crystals in a back-to-back configuration, with ^{22}Na source positioned between the two detectors. MCP PMTs and the crystals are enclosed in plastic support frames, which are fully open in the source direction.

3. Experimental set-up

The experimental set-up consisted of two detector modules in a back-to-back configuration, separated by 140 mm, with a ^{22}Na point source positioned between them (Fig. 1). The PbF_2 crystals [14] were coupled with optical coupling grease to Hamamatsu 16 channel MCP PMTs, with an active surface area of 23×23 mm^2 and 1.5 mm thick borosilicate windows (prototypes based on the MCP PMT presented in Ref. [15]). The pairs of unsegmented crystals used for these measurements were $25\times 25\times 15$ or $25\times 25\times 5$ mm^3 in volume. The surfaces of the crystals were polished and were either wrapped in white reflective Teflon tape or painted black. In this study, only two channels per MCP PMT, located near the center of the device, were read out individually. The signals from the other 14 channels of each MCP PMT were summed into two channels and used to suppress crosstalk background in the two individually connected channels, by selecting events where the individually connected channels had the largest charge measurement. The signals were amplified (ORTEC FTA 820A), discriminated (Philips leading edge discriminator model 708) and timed with a TDC (Kaizu Works KC3781A). The pulse charge was measured with a charge sensitive ADC (CAEN QDC V965). The four signals from each MCP PMT were ORed and the

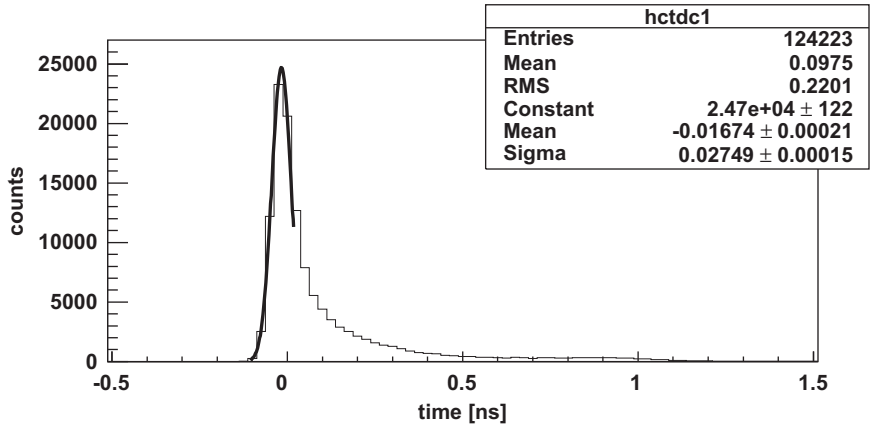

Fig. 2. The time distribution for single photoelectrons obtained for one of the prototype MCP PMT samples. The approximately 1 ns long tail, trailing the main peak, is due to the backscattering of photoelectrons from the front MCP surface. The shape of the distribution is described in more details in Ref. [1].

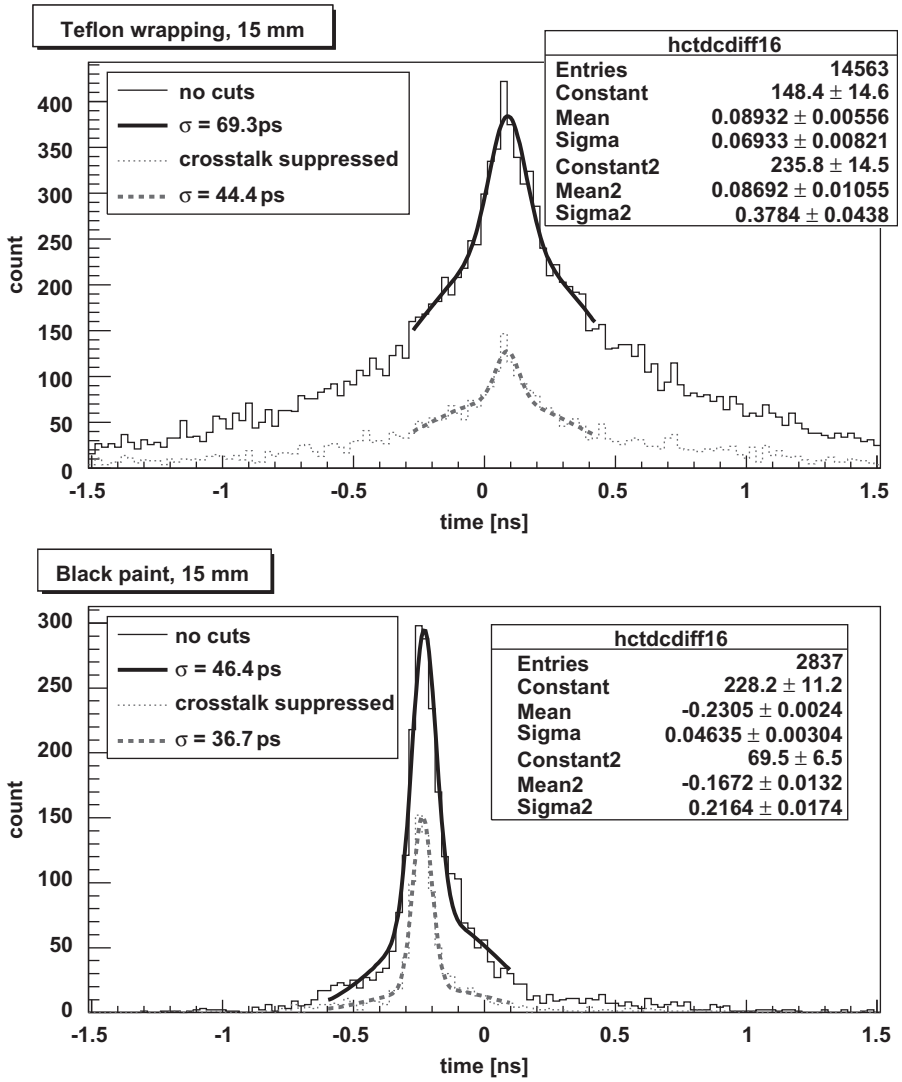

Fig. 3. The coincidence timing distributions obtained with 15 mm thick PbF_2 crystals, in the case of Teflon wrapped (top) and black painted (bottom) surfaces. The histograms of all events (solid line) and the crosstalk suppressed histograms (dashed line, see text for explanation) are fitted with a sum of two Gaussian functions.

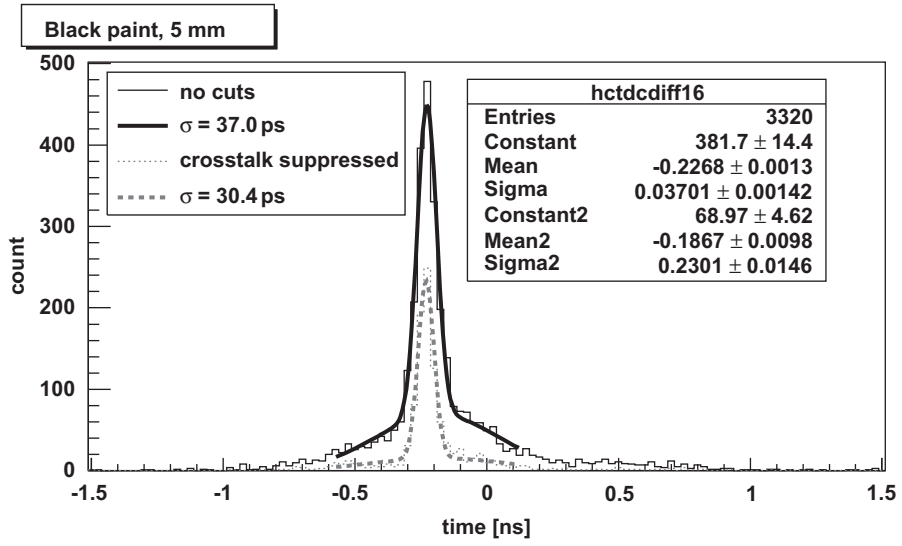

Fig. 4. The coincidence timing distribution obtained with 5 mm thick PbF_2 crystals with black painted surfaces.

Table 2
Experimental results: coincidence time resolutions for different PbF_2 crystals and surface treatments, obtained from the narrow peak of the double Gaussian functions.

	Time resolution σ (ps)	
	Without crosstalk suppression	With crosstalk suppression
15 mm thick, Teflon wrapping	69	44
15 mm thick, black paint	46	37
5 mm thick, black paint	37	30

measurement was triggered by a coincidence between the two resulting signals.

The time resolution of the Hamamatsu MCP PMTs was measured in an independent study by illuminating the MCP PMT with single photon pulses, generated by a PiLas diode laser system EIG1000D. The laser output was attenuated to the single photon level by neutral density filters, while the laser control unit also provided the trigger signal. We obtained an excellent time resolution with $\sigma \approx 27$ ps for both MCP PMTs, which includes the contributions from the laser jitter (15 ps r.m.s.) and electronics (approximately 11 ps r.m.s.). Fig. 2 shows the time distribution obtained for one of the MCP PMTs.

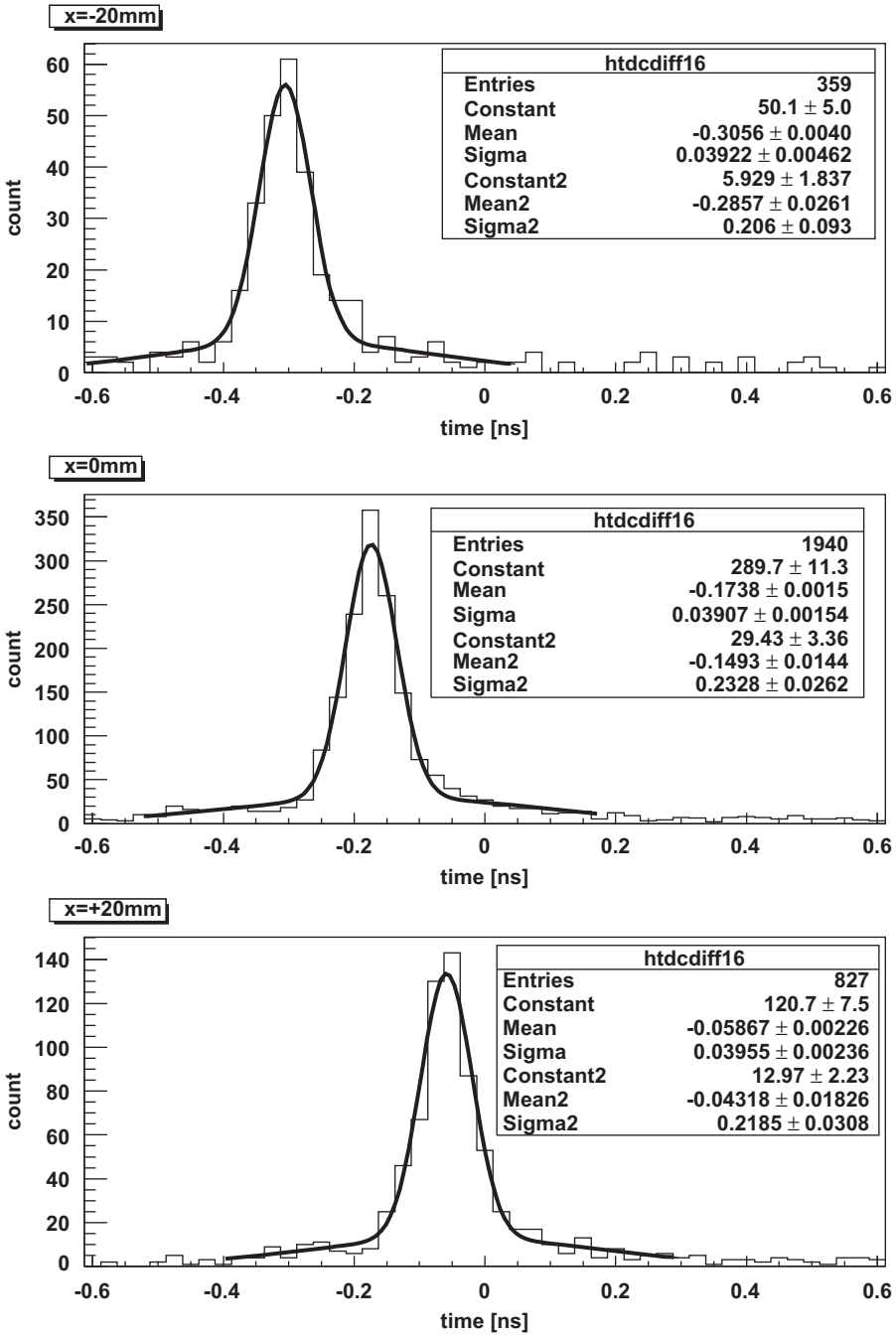

Fig. 5. The coincidence timing distributions obtained with 15 mm thick crystals with surfaces painted black, for the source positioned at −20 mm from the central position (top), for the source in the central position (middle) and for the source positioned at +20 mm from the central position (bottom).

4. Measurements

The corrections for leading edge discrimination time-walk were obtained from a correlation of the pulse time versus pulse height and applied to the TDC measurements. The coincidence timing distributions were obtained by histogramming the difference in corrected pulse arrival times from two selected individually connected channels. The MCP PMTs used in our measurements exhibit some crosstalk between the anode channels [1], which can lead to delayed detection of fake signals on channels neighboring the channel with the true hit. To demonstrate improvements possible by suppressing crosstalk, Figs. 3 and 4 also include histograms containing only the events where both selected channels had the maximum charge of their MCP PMT.

Fig. 3 shows the coincidence timing distributions obtained with 15 mm thick PbF_2 crystals. Painting the surfaces of the crystal black, instead of wrapping them in Teflon, removed the wider contributions, corresponding to photons which undergo one or more reflections before reaching the photodetector. The narrow peak which is due to the photons that reach the photodetector without any reflections remained. This resulted in a significant improvement in the time resolution (Table 2). The remaining tails are mainly due to the backscattering of photoelectrons from the front MCP surface (Fig. 2 and Ref. [1]).

We obtained further improvement in time resolution by using thinner crystals, as shown in Fig. 4 for 5 mm thick PbF_2 crystals with black painted surfaces. Reducing crystal thickness reduces the variation in photon travel times at the expense of gamma absorption efficiency. Some coincidences are also due to detection of Cherenkov photons produced in the 1.5 mm thick borosilicate windows of the MCP PMTs. According to our Monte Carlo simulation, the fraction of such events is below 10% even in the case of 5 mm thick crystals.

To demonstrate how the excellent time-of-flight resolution of the detector can be used for source position reconstruction, we also performed measurements with 15 mm thick crystals, when the ^{22}Na point source was displaced from the central position. Fig. 5 shows the measured time difference distributions for three source positions, spaced by 20 mm along the axis connecting the two detectors. Here, the crosstalk suppressed distributions of time-of-flight difference are used. The average time resolution of the three measurements has $\sigma = 39$ ps, while for the 20 mm shifts the peak position mean value changed by 124 ps on average. This means that we achieved a very good spatial resolution of $\sigma \approx 6$ mm along the line of response only from the time-of-flight measurements.

5. Simulations

The simulations were performed in the GEANT4 framework [16] for a simple back-to-back detector arrangement, corresponding to the set-up used in the experiments. For the estimate of the coincidence time resolution, the active surface area of the photodetector was simulated to be $10.8 \times 10.8\ mm^2$, to take into account the geometric acceptance of the individually connected central channels. For the estimate of the detection efficiencies, the active surface was covering the whole crystal exit surface ($25 \times 25\ mm^2$). The simulation parameters used for crystal properties and photon generation are summarized in Table 1, while Fig. 6 shows the optical transmission curves of PbF_2 and $PbWO_4$ crystals and the photocathode quantum efficiency, used in the simulation. Simulation also included dispersion of the refractive index [11,13]. Teflon wrapping was simulated by a white diffusive reflector.

Table 3 summarizes the simulation results concerning photon production and detector efficiency, while Fig. 7 shows the wavelength distributions of the first detected photons.

The back-to-back timing distributions were obtained as the difference in time between the first photons reaching the central channels of the two photodetectors. The response time spread of the photon detection was not taken into account. The obtained coincidence timing distributions, shown in Fig. 8 for PbF_2 and in Fig. 9 for $PbWO_4$ crystals, were fitted with a sum of two Gaussian functions. The coincidence time resolutions, summarized in Table 4, were obtained as the sigmas of the narrower Gaussian function. Detection efficiencies were calculated as the number of events, where both photodetectors detected at least one Cherenkov photon, divided by the number of 511 keV gamma pairs generated within the detector solid angle.

The results of simulations are in qualitative agreement with our measurements. Black paint on the surfaces of the crystal stops most

Table 3
Simulation results for 15 mm thick crystals: fraction of electrons, which are produced with kinetic energy above the Cherenkov threshold; the average number of Cherenkov photons produced per generated gamma; the average number of Cherenkov photons detected with single photodetector per generated gamma in case of crystals wrapped in white diffusive reflector or painted black.

	PbF_2	$PbWO_4$
Fraction of e^- above Cherenkov threshold	0.77	0.88
Cherenkov photons produced/γ	10.2	15.8
Cherenkov photons detected/γ (white reflector)	0.11	0.068
Cherenkov photons detected/γ (black paint)	0.070	0.044

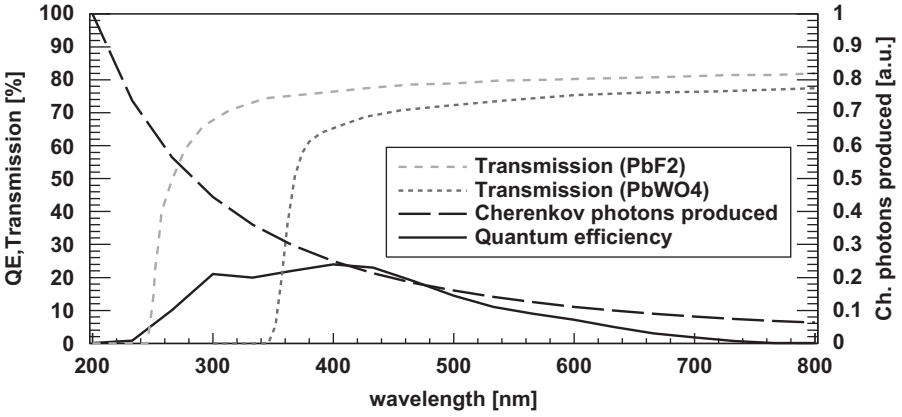

Fig. 6. Wavelength dependence of relevant quantities used in simulation: bialkali photocathode quantum efficiency, optical transmissions of PbF_2 (for 25 mm thick sample, [10]) and $PbWO_4$ (for 230 mm thick sample, [12]) and the $1/\lambda^2$ distribution, which indicates the wavelength dependence of produced Cherenkov photons.

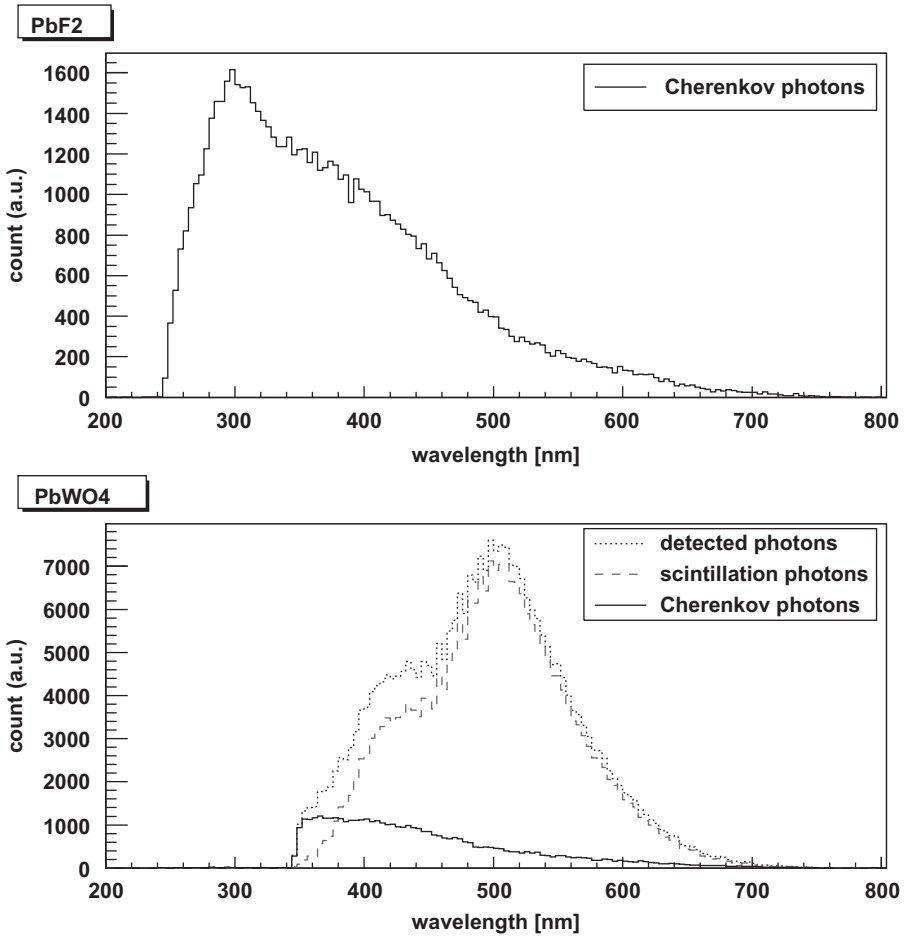

Fig. 7. The wavelength distribution of first detected photons resulting from the simulation, in the case of PbF_2 (top) and $PbWO_4$ (bottom) crystal.

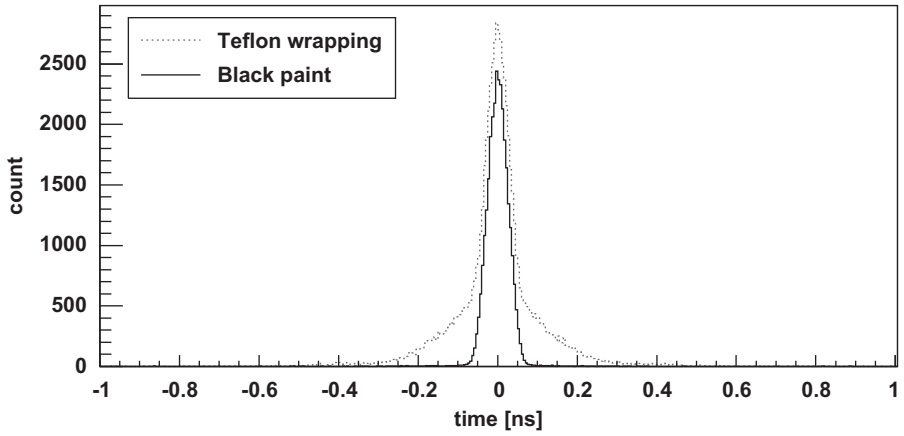

Fig. 8. The simulated coincidence timing distributions for 15 mm thick PbF_2 crystals wrapped in white diffusive reflector (dashed line) and painted black (solid line). These distributions do not include the response time spread of the photodetector.

of the reflections (some total internal reflections remain), leaving only the narrow central peak, corresponding to photons that reach the photodetector without time delays caused by reflections. Although wrapping the crystal in white reflector results in improved efficiency, most of the additional photons are detected with bad timing, since they are reflected. The simulations did not reproduce the long tails of the measurements (Fig. 3), which can be attributed to the photodetector time response, which is not included in the simulations.

The $PbWO_4$ crystal is better than PbF_2 in terms of the number of produced Cherenkov photons (Table 3), due to its higher index of refraction (Table 1). However, because of its higher cutoff wavelength, less photons reach the photodetector. Simulation results obtained with $PbWO_4$ also indicate that the higher index of refraction actually degrades the time resolution, since the Cherenkov photon velocity is lower. Another possible problem with $PbWO_4$ is the scintillation photons, which represent an almost constant background on the time scale of a few ns. According to our simulation, near the central peak this background has approximately the same number of events per 1 ns as there are fast events, produced by Cherenkov photons (Fig. 9).

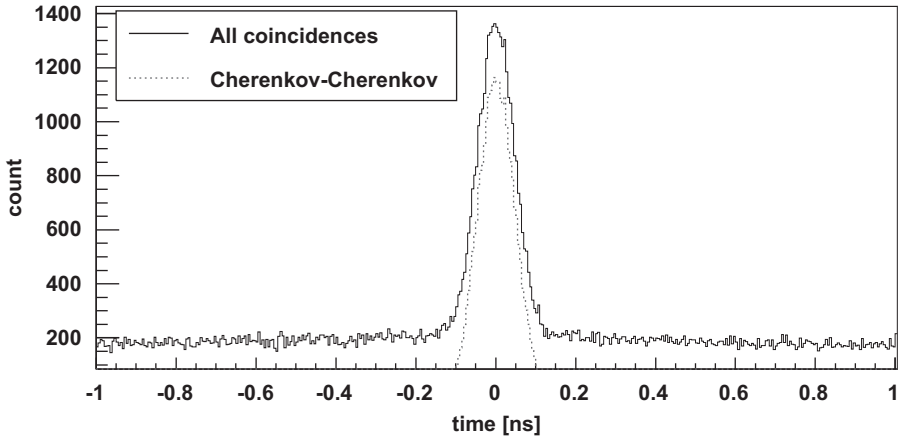

Fig. 9. The simulated coincidence timing distributions for black painted, 15 mm thick $PbWO_4$ crystals. The solid line shows the coincidences produced by any combination of Cherenkov or scintillation photon detection. The dashed line shows the coincidences, caused by detection of Cherenkov photons on both photodetectors. These distributions do not include the response time spread of the photodetector.

Table 4
Simulation results: coincidence timing resolution, only including Cherenkov photon travel time variation (σ_{photon}), also including photodetector time response of $\sigma = 22$ ps (σ_{total}), and coincidence detection efficiency. The efficiencies of $PbWO_4$ include only Cherenkov photons without the scintillations.

	σ_{photon} (ps)	σ_{total} (ps)	Efficiency
PbF_2, 15 mm, white reflector	28	42	1.76
PbF_2, 15 mm, black paint	25	40	0.75
PbF_2, 5 mm, black paint	13	34	0.32
$PbWO_4$, 15 mm, black paint	44	54	0.27
$PbWO_4$, 5 mm, black paint	19	36	0.08

Since scintillation events are indistinguishable from Cherenkov events and are characterised by worse timing, they unavoidably degrade the timing resolution.

6. Conclusion

The use of prompt Cherenkov photons for time-of-flight PET is very attractive, especially with a very fast photodetector, such as the MCP PMT. However, for 511 keV gamma detection the very low number of photons produced in available Cherenkov radiators presents a challenge. The timing resolution obtainable is so good that the photon travel time variation in the crystal becomes the most important contribution. For the best possible timing, photon reflections need to be suppressed by painting the crystal surfaces black, which in turn reduces the number of photons available for detection. Our GEANT4 simulations show that the majority of events are produced by single Cherenkov photons being detected with the photodetectors.

Using two Hamamatsu MCP PMTs in a back-to-back configuration we measured a coincidence timing resolution of $\sigma = 30$ ps (71 ps FWHM) with 5 mm thick and $\sigma = 37$ ps (95 ps FWHM) with 15 mm thick PbF_2 crystals painted in black. Such an excellent timing resolution enabled us to demonstrate a spatial resolution of $\sigma \approx 6$ mm along the line of response.

Admittedly, the efficiency of a detector with an improved timing resolution would be rather low (as seen in Table 4). It was the aim of the present work to investigate mainly the achievable timing resolution and to proceed later on, in a second stage, to optimize other detector parameters. We believe that there is room for improvement of the efficiency. Namely, a superior efficiency could be obtained with a super bialkali photocathode, by using a PMT with a high transmission quartz window and with a Cherenkov radiator transparent down to wavelengths of about 160 nm. In addition, an excellent timing resolution localizes the positron emitting nucleus to about 6 mm r.m.s. along the line of response, therefore introducing a large improvement of image quality. By using a suitably modified reconstruction method, this might require less statistics for a comparable image, thus compensating to a degree the reduced efficiency. Investigations of all these effects are in progress and we hope that this work will stimulate further research, also of other groups, with the aim at the end, of producing a PET apparatus with improved performance.

References

[1] S. Korpar, et al., Nucl. Instr. and Meth. A 595 (2008) 169.
[2] M. Akatsu, et al., Nucl. Instr. and Meth. A 528 (2004) 763.
[3] S. Korpar, et al., Nucl. Instr. and Meth. A 572 (2007) 432.
[4] J. Vavra, et al., Nucl. Instr. and Meth. A 595 (2008) 270.
[5] K. Inami, et al., Nucl. Instr. and Meth. A 560 (2006) 303.
[6] M. Miyata, et al., J. Nucl. Sci. Technol. 43 (2006) 339.
[7] R. Dolenec, et al., in: Proceedings of the IEEE Nuclear Science Symposium, Knoxville, USA, October 28–November 7, 2010.
[8] P. Lecoq, et al., IEEE Trans. Nucl. Sci. NS-57 (2010) 2411.
[9] Producer's specifications 〈http://www.siccas.com/〉.
[10] P. Achenbach, IEEE Trans. Nucl. Sci. NS-48 (2001) 144.
[11] D.F. Anderson, et al., Nucl. Instr. and Meth. A 290 (1990) 385.
[12] A.A. Annenkov, et al., Nucl. Instr. and Meth. A 490 (2002) 30.
[13] S. Baccaro, et al., Nucl. Instr. and Meth. A 385 (1997) 209.
[14] The Shanghai Institute of Ceramics and Chinese Academy of Sciences (SICCAS).
[15] K. Inami, et al., Nucl. Instr. and Meth. A 592 (2008) 247.
[16] S. Agostinelli, et al., Nucl. Instr. and Meth. A 506 (2003) 250.